PROCEEDINGS OF SPIE

Breast thermography: a non-invasive technique for the detection of lesions

L. B. Alvarado-Cruz, C. Toxqui-Quitl, J. A. Hernández-Tapia, A. Padilla-Vivanco

SPIE.

Breast thermography: a non-invasive technique for the detection of lesions

L. B. Alvarado-Cruz, C. Toxqui-Quitl, J. A. Hernández-Tapia, and A. Padilla-Vivanco

Computer Vision Laboratory, Universidad Politécnica de Tulancingo, Ingenierías 100. Col. Huapalcalco, Tulancingo, Hidalgo, México. C.P. 43629.

ABSTRACT

Breast thermography uses ultrasensitive infrared cameras to produce high resolution images of temperatures and vascular changes. In the present work we propose the development of computational methods that allow the analysis and digital processing of breast thermographic images for the detection of regions related to a probable lesion. A semi-automated segmentation algorithm is presented by means of polynomial curve fitting for the detection a region of breast (ROI). A public database which contains information on volunteers with diagnose made by mammography and biopsy is used.

Keywords: Thermal imaging, image segmentation, breast thermography, image description.

1. INTRODUCTION

Breast cancer is currently a condition that mainly affects women. In addition to existing detection methods (mammography and biopsy), there is another complementary technique called infrared thermography[1] that aims to increase the probability of early this condition detection.

Infrared thermography monitors the physiological changes that occur in the breast. Conventional detection methods such as mammography are used after the age of 40. Infrared thermography offers the great advantage of being used in women under 40 years of age. It is also non-invasive, non-ionizing, painless and according to studies performed, it allows locating a tumor of 10 mm - 30 mm in diameter.[2]

Thermograms are usually acquired from a person´s torso, which makes it necessary to use segmentation techniques for the region of interest. The ROI is the adjustment of the limits of the area to be analyzed: right breast and the left breast.[3]

Several works have been carried out[1] that allow the segmentation of the ROI. In different studies, the first stage of segmentation is exposed manually and depends on the expert capturing the image. In other studies semiautomatic or automatic segmentation is proposed, using form finders[1] , Hough transformation and detection operators of edges like the Canny operator. In their research study J. Josephine Selle et al.,[4] present the automated recognition of the ROI for breast thermograms considering the lateral and frontal view of the breasts.

In this paper we describe a semi-automatic ROI segmentation method for thermal symmetry analysis in mammary thermograms. From the ROI it is possible to obtain a map of temperature changes with respect to the average temperature. Section 2 describes the techniques of digital preprocessing of images applied to thermograms. In section 3, the ROI extraction algorithm is presented. The results obtained are summarized in Section 4. Finally, Section 5 presents the conclusions of this work.

A.A.A.: E-mail: laura.alvarado.1631026@upt.edu.mx.
Telephone: (+52) 7761155738.

2. IMAGE ENHANCEMENT

2.1. Gray level transformations

For a transformation T in a neighborhood of size 1×1 (a single pixel), the $g(x, y)$ value only depends on the intensity values and not explicitly on (x, y). The intensity transformation functions frequently are written in a simple form,[5]

$$s = T(r) \tag{1}$$

where r denotes the intensity of f and s the intensity of g, both at any corresponding point (x, y) in the images. Let r be a digital image of $M \times N$ pixels, whose increment in contrast is given through a transformation in intensities such as,

$$s(r, m, E) = \frac{255}{1 + \left(\frac{255 \cdot m}{r}\right)^E} \tag{2}$$

In Fig. 1 the function $s(r, m, E)$ is plotted for the improvement of images with different parameters m and E.
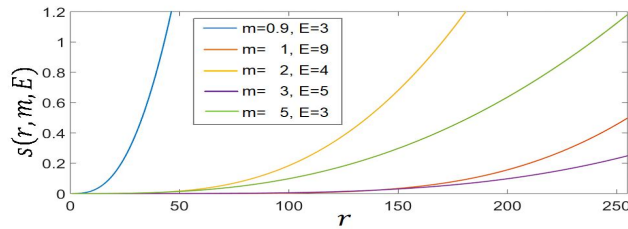

Figure 1. Function of gray level transformations used in the improvement of images.

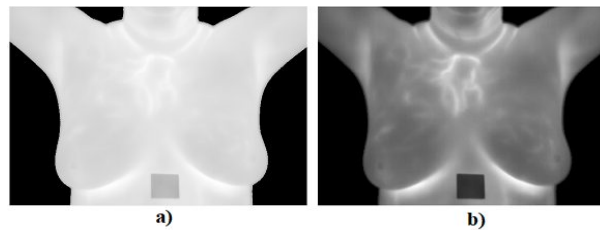In Fig. 2 an example of contrast enhancement to a thermal image is observed.

Figure 2. a) Original image f (x, y), b) image g (x, y) with contrast increase m = 0.9 and E = 3.

2.2. Sharpening images

The first-order derivative of a function $g(x, y)$ is approximated by the difference,

$$e(x, y) = \nabla^2 g(x, y) = \frac{\partial^2 g(x, y)}{\partial x^2} + \frac{\partial^2 g(x, y)}{\partial y^2} \tag{3}$$

A derivative operator is used to find edges in an image and works isotropically on an image function, in such a way that the edges are located enhancing the discontinuities in the gray levels.

3. SEMI-AUTOMATIC SEGMENTATION METHOD

3.1. Horizontal projection profile (HPP) method

The histogram of a digital image with L total possible intensity levels in the range $[0, 255]$ is defined as the discrete function,[2]

$$h(r_k) = n_k \tag{4}$$

where r_k is the k-*th* level of intensity in the interval $[0, 255]$ and n_k is the number of pixels in the image whose intensity level is r_k.

A horizontal projection profile is a histogram of one dimensional array with a number of entries equal to the number of white pixels in each row, and is defined as,

$$hpp(x) = \sum_{y=0}^{N=-1} h(r_k(x, y)), \tag{5}$$

The lower inframammary limit is determined by,

$$Lim_{\text{inf}} = máx\{hpp(x)\} \tag{6}$$

for $x = M - 1, ..., 0$.

Fig. 3 shows an example of the digital processing of a breast thermogram, the inframammary limit found is $Lim_{\text{inf}} = 365$.
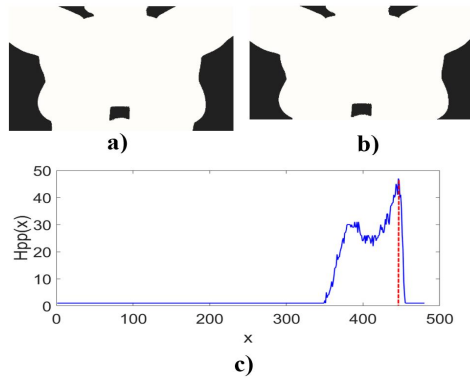

Figure 3. a) Binarized thermogram b) thermogram o(x, y) cut to the lower inframammary limit c) graphic horizontal projection profile.

3.2. Polynomial curve fitting

From the thermogram $e(x, y)$ of Fig. 4a, a set of n points is selected as,

$$(x_1, y_1), (x_2, y_2), ..., (x_m, y_m) \in e(x, y) \tag{7}$$

The data fitting is implemented with a cubic degree polynomial, described in the following equation,

$$f(x) = a_0 + a_1 x^1 + a_2 x^2 + a_3 x^3 \tag{8}$$

where a_0, a_1, a_2, a_3, are coefficients of the polynomial and are determined by the solution of linear equations.[6] Fig. 4b is shows the resulting curves of the polynomial adjustments of degree 3 in addition to the point of intersection that separates the right breast from the left breast.
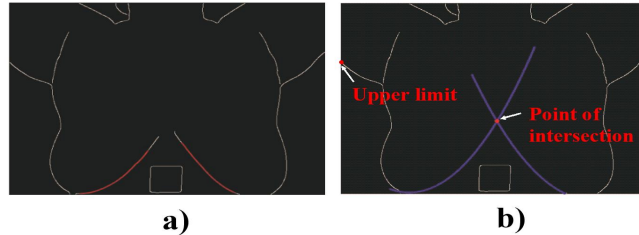

Figure 4. a) Selection of the n points marked in red that will be used for the polynomial adjustment. b) adjustment of n points (x, y) with a cubic-degree polynomial and determination of the intersection point.

3.3. Segmentation of right and left breast for asymmetry analysis

In Fig. 5 the segmentation process of the ROI is shown. Initially, a digital image mask (x, y) of size $M \times N$ pixels was created when calculating the area under the detected curves of Fig. 4b.

Therefore, the ROI segmentation is extracted by,
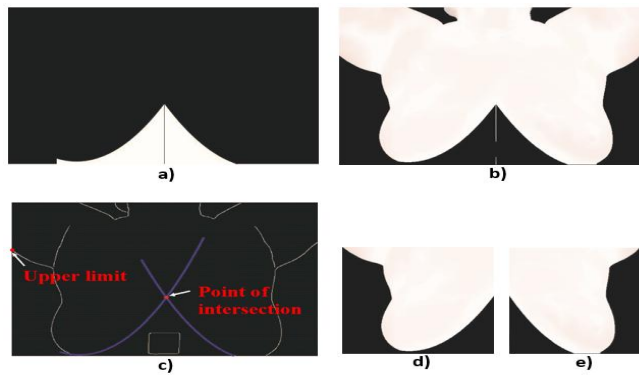
$$seg(x, y) = o(x, y) \cdot maskbin(x, y) \tag{9}$$

Figure 5. a) Digital image mask (x, y). b) segmentation of breast seg (x, y). c) upper limit detection. d), e) separation of the breasts, md (x, y) and mi (x, y).

The number of the row corresponding to the first maximum is taken as the upper limit for the segmentation of the breast thermogram. In this way, the right breast and left breast are separated.

4. RESULTS OF BREAST THERMOGRAM CHARACTERIZATION

4.1. Calculation of average body temperature

The average temperature of a person is obtained by the following expression,[7]

$$p = \sum_{x=0}^{M=1} \sum_{x=0}^{N=1} seg(x, y) \tag{10}$$

$$q = \sum_{x=0}^{M=1} \sum_{x=0}^{N=1} b(x, y) \tag{11}$$

$$\mu_{prom} = \frac{p}{q} \tag{12}$$

where p is the sum of the temperatures of the segmented image $seg(x, y)$, q is the total number of pixels in which temperatures of binary image are and μ_{prom} is the average body temperature of the person. This data can be used later for the description and classification of thermograms.

4.2. Quadrants of the breast

The breast is divided into 6 parts according to frequent locations of cancer apperance as seen Fig 6. Most of the malignant tumors of the breast, approximately 50% take place where the largest amounts of ducts is located in the upper external quadrant of the breast (near to the armpit).[7, 8]
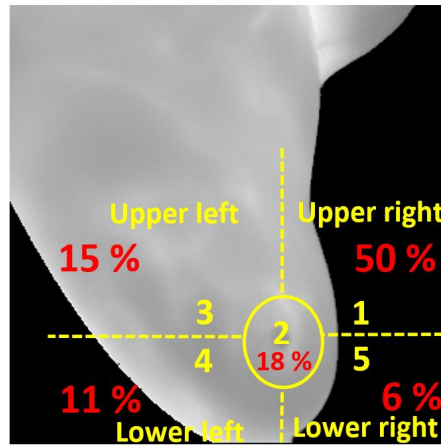

Figure 6. Quadrants in which the breast is divided by amount of tissue and probability of cancer apperance.

4.3. Breast thermogram characterization

A set of 26 thermograms are analyzed. The public database Database For Mastology Research (DMR) is an online platform that stores and manages mastologic images for early detection of breast cancer. The images available in this database are mammography images thermal images with right and left side view and front view. DMR also contains volunteer information such as age, diagnosis made by mammography and biopsy.[9]

Figs. 7 and 8 show thermograms of the public database of Visual Lab of the Federal Fluminense University of Brazil. They are labeled as healthy and unhealthy respectively.

The thermogram was segmented with the method proposed in section 3. The temperature changes Δt are grouped as it follows:[7]

- Class 1 (red), shows an increase of temperature of $\Delta t \geq 3°C$ in relation to μ_{prom}. This increase greater than or equal to 3 °C compared to normal tissue is associated with a malignant lesion.
- Class 2 (yellow) shows temperatures that expose an increase between $1.5°\ C$ and $3°C$ in relation to μ_{prom}.
- Class 3 (blue) shows present increases of $\Delta t = 1.5°C$ with respect to μ_{prom}.
- Class 4 (green) shows temperature increases below $\Delta t < 1.5°C$.
- The black color represents the bottom zone or outside the ROI.

Each thermogram is characterized by a descriptor vector as:

d(1)   Maximum temperature of the left $mi(x, y)$ and right $md(x, y)$ breast.

d(2)   Mean body temperature μ_{prom}.

d(3)   Maximum temperature difference $\Delta t_{máx}$.

d(4)   Area of the region with $\Delta t \geq 3°C$.

d(5)   Breast quadrant location.

Table 1. Characteristics obtained from a thermogram labeled healthy.

Right breast	Left breast
Mean body temperature $\mu_{prom} = 30°C$	
$\mathbf{\Delta t}_{máx}$= **4.1**	$\mathbf{\Delta t}_{máx}$= **4.6**
$\mathbf{t}_{máx}$= **35.4°C**	$\mathbf{t}_{máx}$= **33.4°C**
area = 4584 **pixels**	*area* = 2489 **pixels**
quadrant = **Outside the ROI**	*quadrant* = **Outside the ROI**

Fig. 7 shows a thermogram of a healthy breast, segmented with the proposed method. This thermogram presents a thermal symmetry, it does not reflect an abnormality through the representation of colors. Temperatures exceeding 3°C above the average body μ_{prom} were found. However, it is not located in the area where most malignant tumors occur (right upper quadrant near the armpit).
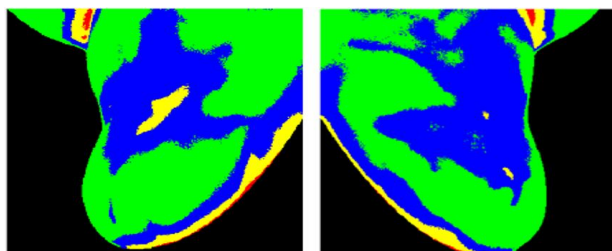
(a)   **(b)**

Figure 7. Thermogram labeled as healthy represented by increases in temperature whit respect to the average temperature in the class: (red) $\Delta t \geq 3°C$; (yellow) $1.5°C < \Delta t < 3°C$; (blue) $\Delta t = 1.5°C$ and (green) $\Delta t < 1.5°C$.

Table 2. Characteristics obtained from a thermogram labeled unhealthy.

Right breast	Left breast
Mean body temperature $\mu_{prom} = 29.9°C$	
$\mathbf{\Delta t_{máx}} = \mathbf{4.6}$	$\mathbf{\Delta t_{máx}} = \mathbf{4.9}$
$\mathbf{t_{máx}} = \mathbf{34.5°C}$	$\mathbf{t_{máx}} = \mathbf{34.8°C}$
$area = 6084$ **pixels**	$area = 16560$ **pixels**
$quadrant = \mathbf{1}$	$quadrant = 1$

The thermogram shown below was classified, according to the diagnosis in DMR, as unhealthy. It is evident that the thermogram is thermally asymmetric, the left breast presents an abnormal pattern as illustrated in Fig. 8 (b). More than one region with temperatures above $3°C$ in relation to μ_{prom} was found. The region with the highest temperature has a maximum difference of $4.9°C$ above $\mu_{prom} = 29.9°C$. It is located in quadrant 1 of the left breast, with a region size of 16560 pixels. However, there were temperatures above $3°C$ in all the quadrants.
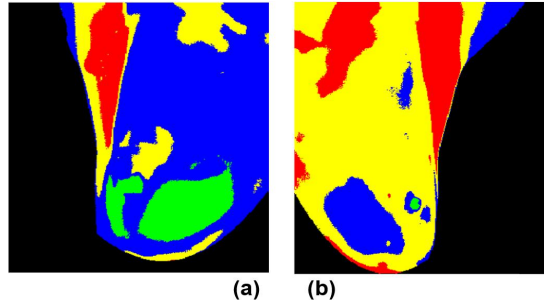

(a)   **(b)**

Figure 8. Thermogram labeled as unhealthy represented by increases in temperature whit respect to the average temperature in the class: (red) $\Delta t \geq 3°C$; (yellow) $1.5°C < \Delta t < 3°C$; (blue) $\Delta t = 1.5°C$ and (green) $\Delta t < 1.5°C$.

5. CONCLUSIONS

In this work, 26 mammary thermograms of a public database were analyzed. Because the thermograms analyzed have a low resolution their analysis is difficult, there are no clear boundaries between regions and the amorphous nature of the object of interest. Therefore, techniques were used to improve contrast, which allow the enhancement of clear limits. The parameters used in the algorithm for the increment in the contrast were $m = 0.9$, $E = 3$ for the entire database.

The extraction of the region of interest was determined by means of the horizontal projection profile method and the adjustment of polynomial curves for the location of the inframammary curves.

Each thermogram was characterized by a descriptor that facilitates the delimitation of the region that presents changes in temperature, represented by colors. The results obtained using the techniques described in this work are compared with the previous classification information of the same database. Therefore, the same results were achieved, that is, the thermograms were correctly classified.

6. ACKNOWLEDGEMENT

REFERENCES

[1] Tiago B. Borchartt, A. Conci, R. C.F. Lima, R. Resmini, A. Sanchez, "Breast Thermography from an image processing viewpoint: A survey Signal Processing". Signal Processing, **93**(10), 2785-2803 (2013).

[2] Dayakshini Sathish, Surekha Kamath, Keerthana Prasad, Rajagopal Kadavigere Roshan J. Martis, "Asymmetry analysis of breast thermograms using automated segmentation and texture features". Signal, Image and Video Processing ,**11**(4),745–752 (2016).

[3] Rodríguez Guerrero, S., & Loaiza, H., & Restrepo Girón, A. "Automatic segmentation of thermal images of the breast to support the detection of cancer". Systems & Telematics, **12** (30), 25-34 (2014).

[4] J. Josephne Selle, A. Shenbagavalli, N. Sriraamb, B. Vemkatraman, M. Jayashreedand, M. Menaka. "Automated recognition of ROIs for breast thermograms of lateral view-a pilot study". Quantitative InfraRed Thermography Journal,**11**,1768-6733 (2018).

[5] Gonzalez and C, Rafael and , Woods and E, Richard and , Eddins and L, Steven," Digital Image Processing Using MATLAB". Prentice Hall , 2nd ed., (2009).

[6] Raymond P. Canale and Steven C. Chapra,"Métodos Numéricos para ingenieros". Mc Graw Hill, 6ed., 417-432 (2011).

[7] O. A. Zermeño Loreto, E. E. Orozco Guillén, C. Toxqui Quitl, A. Padilla Vivanco, "Characterization of images in the infrared spectral region for the detection of lesions in the breast". Cathedra, **6**(2), 75-82 (2017).

[8] http://www.needgoo.com/anatomy-of-the-breast/ "Anatomy of the Breast and common cancer areas"., (2012) (Accessed September 4, 2017).

[9] Silva, L. F., Saade, D. C. M., Sequeiros, G. O., Silva, A. C., Paiva, A. C., Bravo, R. S., Conci, A., "A New Database for Breast Research with Infrared Image ". Journal of Medical Imaging and Health Informatics, **4** (1), 92-100 (2014).